Available online at www.sciencedirect.com
SCIENCE DIRECT
Polymer 47 (2006) 3814–3825
polymer
www.elsevier.com/locate/polymer

The phase mixing studies on moisture cured polyurethane-ureas during cure

D.K. Chattopadhyay [a], B. Sreedhar [b], K.V.S.N. Raju [a,*]

[a] Organic Coatings and Polymers Division, Indian Institute of Chemical Technology, Taranaka, Hyderabad 500 007, India
[b] Inorganic and Physical Chemistry Division, Indian Institute of Chemical Technology, Hyderabad 500 007, India

Received 23 August 2005; received in revised form 21 February 2006; accepted 18 March 2006

Abstract

Moisture cured polyurethane-urea (MCPU) is one of the industrially important polymers that shows good thermal, mechanical and weathering properties and is widely used in the reactive hot melt adhesives and coatings. Structural variation of the building blocks, i.e. soft, hard segment and chain extender structure on the phase mixing characteristics during cure in polyether based moisture-cured polyurethanes (MCPUs) has been investigated. Variations in the soft segment structure like polyethylene glycol (PEG), polypropylene glycol (PPG) and polytetramethylene glycol (PTMG) and hard segment like toluene diisocyanate (TDI) or isophorone diisocyanate (IPDI) were made. The effect of isocyanate content (NCO:OH ratio 1.6:1 and 2:1) as well as various aliphatic diol and aromatic diamine chain extenders were also compared. The phase mixing phenomenon during network growth was evaluated by differential scanning calorimetry (DSC) and a correlation was drawn for the degree of cure with the phase mixing property. The change in modulus and thermal stability with the cure advancement were measured by dynamic mechanical and thermal analysis (DMTA) and thermogravimetric analysis (TGA). A correlation was made for the soft, hard segment and chain extender structure to the phase mixing phenomenon during cure. The rate of phase mixing was found to be dependent on the subtle variations in molecular architecture.

Keywords: Polyurethane; Moisture cure; Phase mixing

1. Introduction

Moisture cured polyurethane-ureas (MCPUs) are widely used in the sealant production, high performance coating sector as well as reactive hot melt adhesive industries. They provide the functional groups necessary for curing with atmospheric moisture. The attractive mechanical properties of MCPUs results from the microphase-mixed morphology brought about by the solid state posture reaction of the hard segment. Partial mutual insolubility of different chemical sequences in the block copolymer results in biphasic morphology. One of the microphases is derived from the macrodiol and is generally referred to as the soft micro-domain or phase that imparts softness and extensibility. It is relatively immiscible with the other phase derived from the diisocyanate and chain extender and is referred as hard micro-domain or phase, which provides cohesive strength to the polymer matrix. During the urea network maturation, soft and hard microphase mixes, and provides a delicate balance between the phase mixing and phase separation. Therefore, by suitable variation in chemical structure, composition and synthetic conditions, it is possible to obtain tough, high-strength polymer with an extremely wide range of mechanical and thermal properties. In fact, it is this tremendous ability to readily modify the properties of these materials by variation in chemical structure and composition that has stimulated the enormous technological and scientific interest in these polymers. Thus, in principle, it is possible to tailor the thermal, mechanical, and optical properties of MCPUs to meet specific performance criteria [1].

Cure of MCPU advances with progress of time and produces crosslink networks by the diffusion of moisture, nucleophilic attack and generation of primary amine that further react to produce urea bonds [2,3]. As the chemical reaction proceeds, urea chain length increases and the interaction parameters between the polyether soft and polyurea hard segment also changes. Such changes lead to a transition from an initially homogeneous state into a microphase mixed state. The major drawback of MCPU coatings is the formation of side products on storage and if these reactions are significant, both pot stability and shelf life are expected to be dramatically affected. The presence of side products, for example allophanate

* Corresponding author. Tel.: +91 4027202080.
E-mail addresses: kvsnraju@iict.res.in (K.V.S.N. Raju), drkvsnraju@yahoo.com (K.V.S.N. Raju).

0032-3861/$ - see front matter © 2006 Elsevier Ltd. All rights reserved.
doi:10.1016/j.polymer.2006.03.092

and isocyanurate, add branch points, which increases the viscosity of the NCO capped prepolymer and changes the onset of gelation during cure and thereby lower the storage stability of the product [4–7]. The presence of additional hard segment material due to biuret and allophanate changes the hard domain volume fraction and hence the interconnectivity of the hard segments [8], alter the thermal properties [9,10] as well as adhesive behaviour [11].

The degree of microphase mixing and the overall texture is dependent on factors such as hard–soft segment composition ratio, the average length of each segment, soft and hard segment structure, the solubility parameter and crystallizability of each segment, crosslinking in either phase and the overall molecular weight [3]. Accordingly the properties of MCPU can be custom tailored by introducing controlled changes in polyol chain length as well as by changing the proportions and chemical nature of constituents, which make up the flexible and rigid segments of the polymer chain. The long-term performance, including dimensional stability and durability of the coating is strongly dependent on the network structure and the degree of curing. Information regarding cure process and development of macroscopic properties is essential, such that an objective description of the events taking place and, ultimately, selective control of the process and properties can be achieved. The process of curing defines the properties of the finished coating material. Temperature, humidity level and the state of cure are, therefore, key aspects for understanding and controlling the coating performance [12–20]. Yanjun et al. [21] modeled the curing process of isocyanate terminated urethane prepolymer based on oligoester or oligoether diols and diisocyanates by isothermal and non-isothermal DSC under saturated humidity level and have shown a second-order autocatalytic model can be successfully used to evaluate cure process. Comyn and co-workers [22] measured the depth of moisture cure (z) of two reactive hot melt adhesives. Jeong et al. [23] studied the curing kinetics of NCO terminated prepolymer as a function of sample thickness. However, in case of a particular humidity level other than saturated one, the film during the cure has to be evaluated a number of times to obtain any information about the changes in structure on molecular level. The process is time taking and complex in nature, and to our knowledge no reports are available for such changes. The information about isocyanate–water reaction taking place in the system was visualized by monitoring the changes in the sample morphology by DSC, development of macroscopic properties such as modulus development by DMTA and thermal stability by TGA as a function of cure time.

2. Experimental section

2.1. Materials and method

In brief, NCO terminated oligomers were prepared using PEG, PPG and PTMG (Aldrich) in the presence of trimethylol propane (TMP-Aldrich). Fifty grams polyether diol and 9 g TMP mixture was taken and reacted at 80 ± 2 °C with diisocyanate (TDI-Fluka Chemical Corp. NY; 9:1 ratio of 2,4 and 2,6 isomer and IPDI-Aldrich, Z and E isomer in 3:1 ratio) for 6 h in 2-ethoxyethyl acetate (S.D. Fine Chem., Mumbai, India) solvent. The NCO:OH ratio was maintained at 1.6:1 and 2:1. The detailed synthetic process is reported elsewhere [3,19,20].

Table 1
The chemical composition of different MCPUs (amount of TMP was fixed in all the formulation)

Sample name	Composition			
PEG/TMP/TDI	PEG	TDI	NCO:OH-	
PEG/TMP/		IPDI	=1.6:1	
IPDI				
PPG/TMP/TDI	PPG	TDI		
PPG/TMP/		IPDI		
IPDI				
PTMG/TMP/	PTMG	TDI	NCO:OH-	
TDI (1.6:1)			=1.6:1	
PTMG/TMP/			NCO:OH-	
TDI (2:1)			=2:1	
PTMG/TMP/				1,4-Butanediol
TDI/BD				
PTMG/TMP/				2-Butyl 2-ethyl
TDI/BEP				1,3-propanediol
PTMG/TMP/				4,4′-Diamino
TDI/SUL				diphenyl sulfone
PTMG/TMP/		IPDI	NCO:OH-	
IPDI			=1.6:1	

A detailed composition of the various oligomers synthesized is given in Table 1. As the reaction was carried out for 6 h in the absence of any added catalyst, so the product mixture contains diurethane, monourethane and unreacted diisocyanate. In our earlier paper [24], the structural assignments of different protons and carbons associated with different environment in the liquid state were carried out by 1D and 2D homo and hetero-nuclear nuclear magnetic resonance (NMR) experiments, and have shown that after 6 h of reaction the fractional isocyanate conversion was approximately 10–15% for IPDI based formulation. The % NCO conversion for TDI based system showed 35–40% after 6 h as determined by dibutylamine titration.

Synthesized PTMG/TMP/TDI (NCO:OH = 2:1) was chain extended with 1,4-butanediol (BD, Spectrochem Pvt. Ltd, India), 2-butyl 2-ethyl 1,3-propanediol (BEP, Aldrich) and 4,4′-diamino-diphenyl sulfone (SUL, Fluka). The chain extension was carried out from the theoretical excess NCO groups with NCO:OH ratio 2:1 for aliphatic diols and 4:1 for aromatic diamine. The synthesised oligomers were mixed with 0.05 wt% dibutyl-tin diluarate (Aldrich) and 0.05 wt% triethylamine catalysts (S.D. Fine Chem.). The free films with thickness 0.15 mm were obtained after casting on tin foil and amalgamation [19,25] and stored at 25 °C and 45% of relative humidity for evaluation.

2.2. Instruments and cure characterizations

The cure study was carried out periodically with Fourier transform infrared spectroscopy (FTIR), DSC, DMTA and TGA. After each evaluation, the sample was stored at the

prescribed atmosphere until the second evaluation was carried out. FTIR spectra were collected on Nicolate Nexus spectrometer with DTGS TEC detector. A resolution of 4 cm^{-1} and 128 scans were averaged to obtain each spectrum. Calorimetric measurements were carried out on Mettler Toledo 821^e DSC (Zurich, Switzerland) in the temperature range −60 to 200 °C at a heating rate of 10 °C min^{-1} under nitrogen atmosphere (flow rate, 30 mL min^{-1}). The instrument was calibrated with indium standards before measurements. The rescan spectra were acquired after the initial heating the sample from −60 to 200 °C at 10 °C min^{-1}, then cooled to −60 °C at a rate of 50 °C min^{-1}, wait at −60 °C for 20 min and then further scanning the sample at a rate of 10 °C min^{-1} from −60 to 200 °C under nitrogen. DMTA IV instrument (Rheometric Scientific, USA) in tensile mode at a frequency of 1 Hz and heating rate of 3 °C min^{-1} was used to determine the change in sample modulus ($15\times10\times0.15$ mm^3) with temperature in nitrogen atmosphere, and in the temperature range 40–150 °C. The shear mode experiments were carried out at a frequency of 1 Hz, with a heating rate of 3 °C min^{-1} in the temperature range of −80 to 200 °C in nitrogen atmosphere. The thermal stability of polymer films in N_2 environment (flow rate, 30 mL min^{-1}) with the progress of cure was studied on Mettler Toledo TGA/SDTA 851^e instrument in the temperature range 25–500 °C with 10 °C min^{-1} heating rate.

3. Results and discussion

3.1. FTIR analyses

Fig. 1 shows the infrared spectra in the zone 400–4000 cm^{-1} of PTMG/TMP/TDI thin films on KBr disc with cure time. The spectra are mainly characterized by bands at 3150–3600 cm^{-1} (NH stretching vibrations), 2800–3000 cm^{-1} (CH stretching vibrations: anti-symmetric and symmetric stretching modes of methylene groups), 2795 cm^{-1} (O–CH_2 stretching), 1600–1760 cm^{-1} (amide I: C=O stretching vibrations), 1540 cm^{-1} (amide II, $\delta_{N-H}+\nu_{C-N}+\nu_{C-C}$) [26], 1376–1388 cm^{-1} (νC–N), 1226–1292 cm^{-1} (amide III, ν_{C-N}), 1105 cm^{-1} (C–O–C stretching vibration, ether group) and 766 cm^{-1} (amide IV). Band at 1445 cm^{-1} is attributed to CH_2 scissoring and CH_3 deformation. Absorbance in between 1002 and 1012 cm^{-1} is attributed to the stretching and rocking vibrations of the C–C and CH_2 groups, respectively. Amide V appeared at 695 cm^{-1}. The band at 553.5 cm^{-1} is assigned to the δ(N–C–N) by analogy to the case of methylalkylureas [27]. C–O–C and C–C–O bending vibrations appeared at 453.5–455.3 cm^{-1}. Amide I vibration consists of several components reflecting C=O groups in different environments and is sensitive on the specificity and magnitude of hydrogen bonding. Amide I mode is a highly complex vibration and involves the contribution of the C=O stretching, the C–N stretching, and the C–C–N deformation vibrations. Amide II mode is a mixed contribution of the N–H in-plane bending, the C–N stretching, and the C–C stretching vibrations and is sensitive to both chain conformation and intermolecular hydrogen bonding. Amide III mode involves the stretching vibration of the C–N group. Amide III is highly mixed and complicated by coupling with NH deformation modes and is observed between 1226 and 1292 cm^{-1}. Amide IV, V, and VI bands are produced by highly mixed modes containing a significant contribution from the NH out-of-plane deformation mode. They are expected to be in the 800–400 cm^{-1} region [27]. A very weak single band is observed at 838 cm^{-1}, which might be originating either from the coupled vibration of the C–O stretching or CH_2 rocking modes. The strong infrared band assigned to the asymmetric stretching vibration of the C–N group is expected at 1040 cm^{-1}. This band overlaps with the very strong band at 1105 cm^{-1}, the C–O–C stretching vibration of ether groups in PTMG/TMP/TDI [28]. Now let us see the structural changes that occur during the cure reaction. Scheme 1

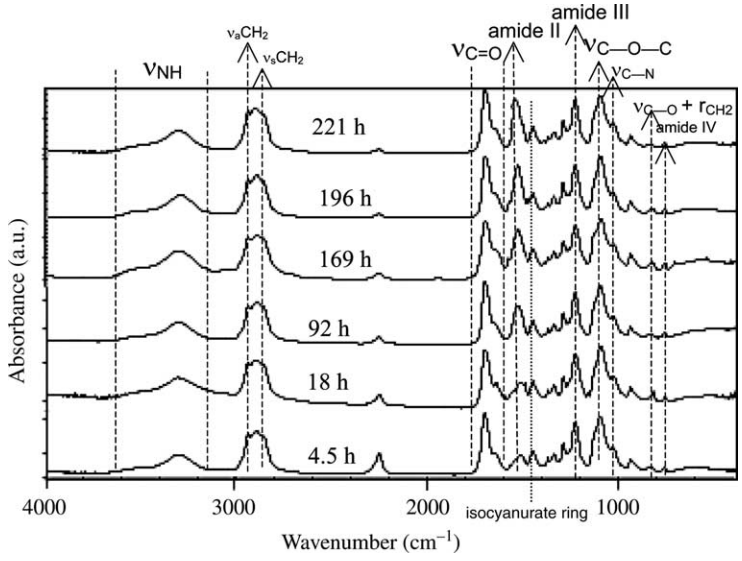

Fig. 1. The representative FTIR spectra of PTMG/TMP/TDI in the zone 400–4000 cm^{-1} (NCO:OH = 1.6:1) with cure time.

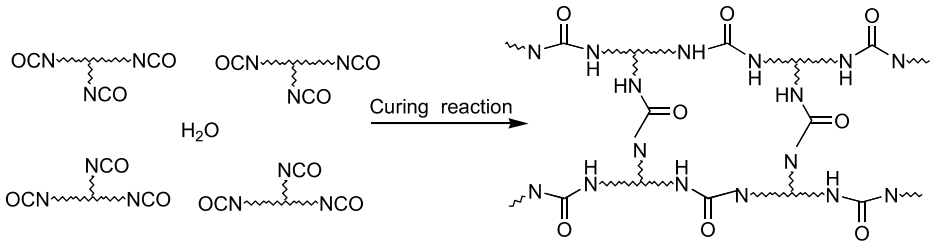

Scheme 1. Cure reaction in the solid state during network advancement.

shows the cure reaction and network development, while Fig. 2(a) shows the decay of NCO group vibration with increasing cure time for PTMG/TMP/TDI system with NCO:OH ratio 1.6:1. The integrated peak areas with increasing cure time suggest that more than 221 h is needed to achieve 95% cure, with an estimating error of $\pm 3\%$. At the same time, the bands due to urea linkages, namely N–H stretching and deformation bands around 3400 and 1525 cm^{-1}, respectively, increase as crosslinking reactions progress. In Fig. 2(b), the NH zone of PTMG/TMP/TDI is shown. The crosslinking reaction during the cure results in a decrease in molecular mobility, therefore, the hydrogen bonding between the donor (N–H group in the urea and urethane linkages) and acceptor (urethane's C=O, urea's C=O or the oxygen atom of the ether linkage) part reduces. Since for stronger hydrogen bonding, the frequency shift ($\Delta\nu$) towards the lower wavenumber region will be higher, therefore, the NH hydrogen bonded stretching vibration at 3410 cm^{-1} was assigned as –NH···O=C (type 1) and a strong absorption peak centered at around 3315 cm^{-1} as –NH···COC (type 2) hydrogen bonds. The peak contribution of type 1 and type 2 hydrogen bonding structure in PTMG/TMP/TDI suggests that the amount of phase mixing was higher compared to the amount of phase separation. The free NH stretching vibration appears at about 3515 cm^{-1}. An overtone of deformation vibration of NH group increased by Fermi resonance at 3185 cm^{-1} was also observed [29]. The conversion, ρ_{NCO} of NCO groups was derived from the equation [23]

$$\rho_{NCO} = (1 - R_{NCO}) = 1 - A_t/A_0 \quad (1)$$

where A_t and A_0 are the integrated absorbance of the NCO stretch band as a function of time, t, and at zero time, respectively. The results of the conversion, ρ_{NCO} of different PTMG soft segmented PU-urea system with cure time is shown in Fig. 2(c). The results demonstrated a slow cure behaviour with increasing NCO:OH ratio as well as a decrease in conversion when IPDI was used as a diisocyanate instead of TDI was observed.

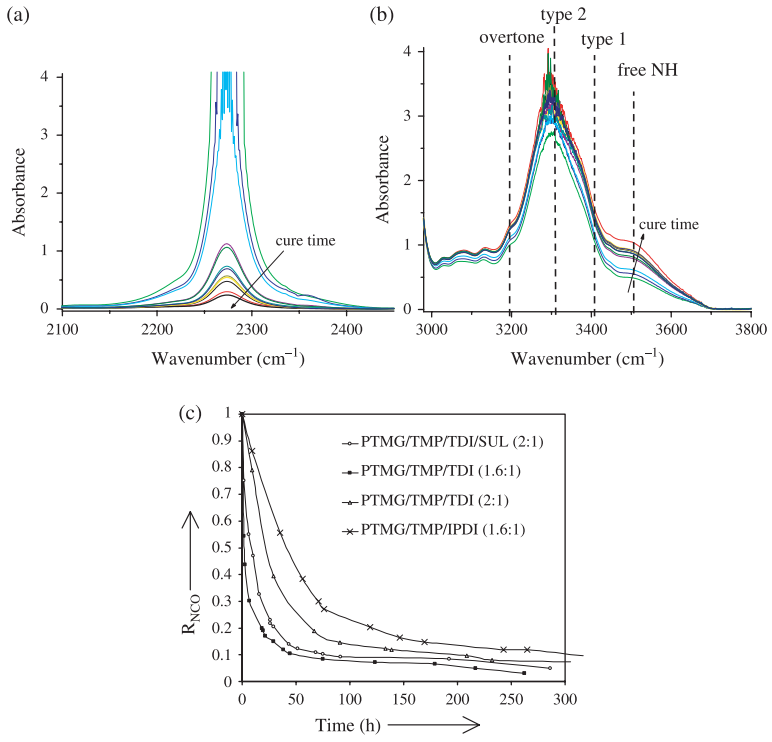

Fig. 2. The representative FTIR spectra of PTMG/TMP/TDI (NCO:OH = 1.6:1) with cure time: 0, 1.3, 2.3, 6.4, 19.3, 18.3, 21.3, 29.3, 38.4, 44.3, 75.1, 123.6, 179, 216.6 and 262.4 h. (a) NCO zone, (b) N–H zone and (c) conversation of NCO group (ρ_{NCO}) as a function of time of PTMG based moisture cured PU-ureas (the direction of arrows in (a) and (b) shows an increasing cure time).

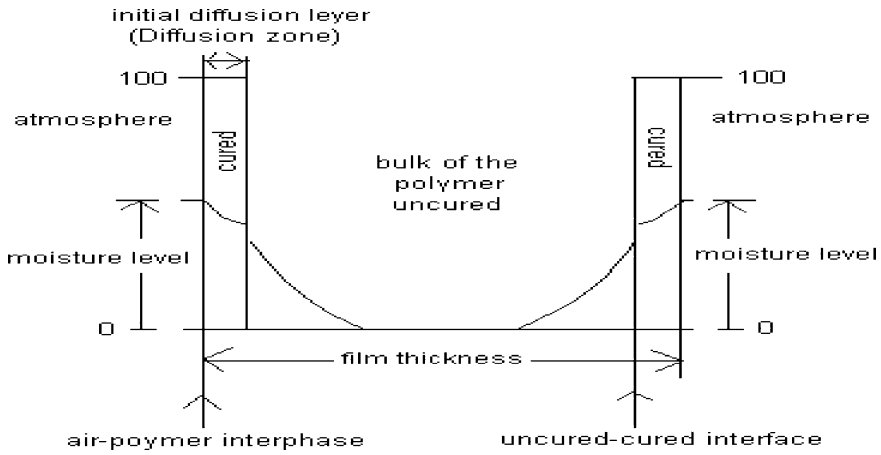

Fig. 3. Schematic moisture profile in the moisture cured PU-urea film.

3.2. DSC analyses

In moisture cured polyurethane, the chemical reactions that take place within the material occur much faster than the rate of water vapor diffusion. Thus, the material may quickly form skins after application and exposure to the air. This skin then acts as a barrier for permeation of moisture into the remaining uncured material inside the bulk. Any water, which passes through the barrier layer quickly reacts with the uncured material and thickness of the barrier increases. Therefore, the moisture content in the film at a certain depth depends on factors such as humidity level in the atmosphere, morphology of the diffusion zone, free isocyanate concentration in the bulk of the polymer and other associated structural factors [30]. The structural developments in these systems occur from two competitive phenomenons, namely thermodynamic phase mixing and kinetics of polymerization. The growth rate follows a diffusion-dominated mechanism and the polyurea formed towards the polymer air interface, i.e. first diffusion layer (Fig. 3) suppress the mobility of water molecules towards the bulk and reduces the polymerization rate. The crosslinking structure formed by the introduction of triol could impede phase separation and produced single broad endotherm in between 40 and 120 °C, which is associated with the enthalpy relaxation phenomena due to the short-range order. Clough et al. [31] interpreted the DTA or DSC endotherm near 80 °C to be the dissociation of hard segment-soft segment hydrogen bonds and Saymour et al. [32] reinterpreted this transition to be morphological in origin. The corresponding rescanned spectra showed no such endotherm (Fig. 4), because no aging time below the hard segment T_g was allowed for the ordering to take place. The hard segment glass transitions were within the broad endothermic zone and were observed in the rescan spectra. The endotherm at the soft segment T_g appeared within two hours of casting the film (Fig. 4) is related to its crystallinity. The decrease and disintegrating of this endotherm suggests the reduction in soft segment crystallinity as a result of phase mixing. With cure time the enthalpy (ΔH) associated with the breakdown of hydrogen bonding between polyurethane/urea groups (NH···O=C, type I) and between the polyurethane/urea groups with ether–oxygens of the soft segment (NH···COC, type 2; Scheme 2) increased and the broadening of the transition took place. The minima in the endotherm, also called peak temperature of the transition, T_{min}, shifted towards high temperature region and transition width (distance between onset and endset of the transition) increased with the progress of cure. The T_m and ΔH values of PPG/TMP/IPDI after 2.5 and 386 h were 59.7 °C, 0.9 J g^{-1} and 81.2 °C, 27.7 J g^{-1}, respectively, (Fig. 4). Crawford et al. [33] and other researchers [32,34,35] in their study on thermoplastic PU elastomers suggested that the endothermic transitions around 60–80 °C (endo I) and above 117 °C (endo II) were associated with the breakdown of hydrogen bonding between the polyurethane/urea–ether bonds, and the breakdown of the hydrogen bonding in between hard segments, respectively. Seymour et al. [36] found that the behavior of endo I strongly dependent on the thermal history and may move continuously upscale in temperature by annealing until it merge endo II. Let us remove the skepticism about the broadening and temperature upscale shift of endothermic transition during cure, which was

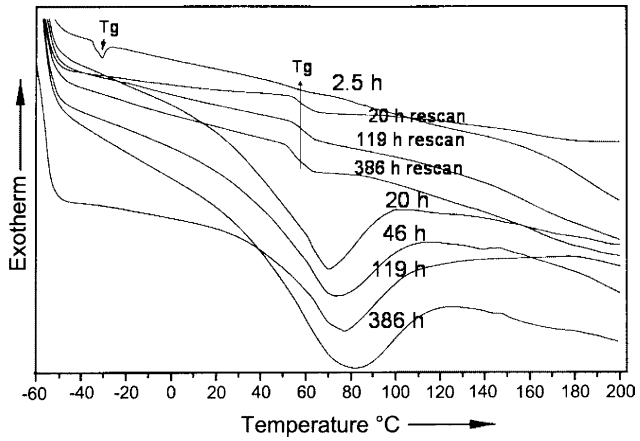

Fig. 4. DSC thermogram of PPG/TMP/IPDI (NCO:OH ratio of 1.6:1) system with cure time shows the changes in T_{min} and ΔH (rescan represents a second scan of the sample carried out with initial heating the sample from −60 to 200 at 10 °C min^{-1}, then cooled to −60 at 50 °C min^{-1}, wait at −60 °C for 20 min and then further scanning the sample from −60 to 200 at 10 °C min^{-1} under dry flow of N_2).

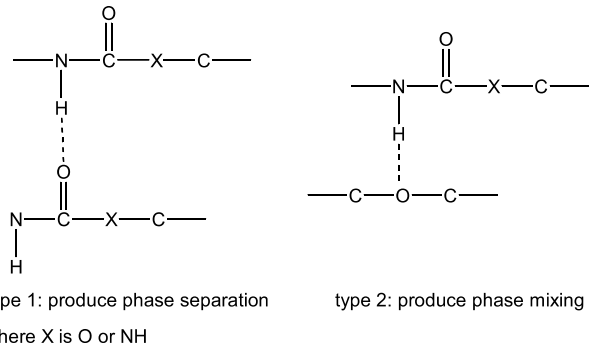

Scheme 2. Two hydrogen bonded structure responsible for phase separation and phase mixing characteristics in the MCPU.

associated with the phase mixing process and not due to the sample thermal history. The higher temperature shifting nature of the endotherm and particularly T_{min} is somewhat confusing, and one may account it according to Crawford [33] observation, as phase separation process associated with increased amount of type 1 hydrogen bonding formation during network advancement. Recently, ab initio calculations along with associated experimental studies have shown that type 2 hydrogen bond is stronger than type 1 bond [37–40]. Ren et al. [41] in their study using energy optimization of different conformers, have shown that in polyether based polyurethane model molecules, NH···COC (type 2; 5.576 kcal mol^{-1}) bond is stronger than NH···O=C bond (type I; 5.430 kcal mol^{-1}) using ab initio calculation and molecular mechanics method with COMPASS force field calculation. They also suggested that the steric volume of the neighboring groups may affect the strength of hydrogen bonds and their studies were in consistent with the earlier observation of hydrogen bonds using vibrational spectroscopy [42–44]. Our observations on the soft segment T_g in the shear mode DMTA analysis suggests the existence of partial phase separation behavior for the postcure material PTMG/TMP/IPDI/SUL and will be addressed later. Considering earlier works [41], the broad endotherm was assigned to the disruption of NH···O=C and NH···COC hydrogen bonds (Scheme 2) and as the bond energy of type 2 bond is more, therefore, increase in the peak temperature (T_{min}) of this transition with the cure time, suggests that the concentration of polyurethane/urea–ether hydrogen bond increased and phase mixing taking place with the network growth. These results are in agreement with the earlier studies, where researchers [38,42] suggested that the interactions, primarily formation of hydrogen bonds, between hard–soft segments are more favorable or stronger than interactions between individual hard–hard components. It could also possible that the phase separation to some extent, from the completely homogenised phase taking place in addition to phase mixing during the network maturation [32–36] and, therefore, results a high strength polymer with delicate balance between phase separation and phase mixing in the completely cured state.

Fig. 5 represents DSC thermograms of PTMG/TMP/TDI (NCO:OH ratio 1.6:1) system with the progress of cure and shows the increase in the ΔH value from 4.9 J g^{-1} at 4.5 h to 35 J g^{-1} at 221 h, T_{min} changes from 63 to 87 °C during this period. Therefore, DSC characterization revealed endotherms with increasing T_{min} during the network maturation and suggests the phase mixing characteristics during the network advancement [45]. A final insight into the phase mixing could be gained from the analysis of the width of the transition, which followed increasing trend with the cure progression. The cure reaction is complicated and does not confine only to the formation of urea bonds. There are other possible hypotheses, given the myriad of side reactions known to be possible in polyurethane chemistry. Once the urea group is formed, it may react with the leftover NCO groups in its vicinity and may form biuret or allophanate by an autocatalytic mechanism. Therefore, the possible formation of crosslink networks by the reaction between urea; urethane and residual isocyanate end groups that result in the formation of biuret and allophanate linkages may affect the resultant outcome [6,7,11]. However, Duff and Maciel [46] reported that, the predominant postcure process is the formation of urea linkage and Dusek et al. [47] shown that the formation of biuret is much faster than allophanate; and at low temperature ($\leq$60 °C) formation of biuret and allophanate is very slow. The presence of such functions may affect the nature of endotherm, thermal stability and overall macroscopic property. Additionally, possibilities of side products formation also exist during the preparation of polyurethane. However, synthesis in solution with controlled atmosphere could result lower molecular weight due to the lack of side reactions that cause branching for IPDI based polyurethane as observed earlier by researchers [24,48], whereas for TDI based PU the possibility of formation of side products cannot be excluded [49]. Again, storage of MCPUs in a completely humid free environment for a long time may result in enhancement in the viscosity due to the formation of side products. Therefore, thin films were casted as soon as the material was prepared and stored in controlled condition for evaluation. For comparison purpose thick film (0.3 mm) of PTMG/TMP/TDI (NCO:OH ratio of 1.6:1) was also casted. The morphology of such PU-urea films significantly depends upon the film thickness [23], because the film

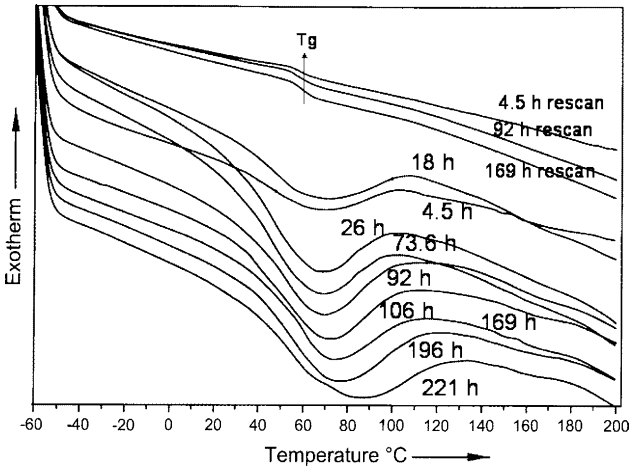

Fig. 5. DSC thermograms of PTMG/TMP/TDI (NCO:OH = 1.6:1) with cure time.

formation mechanism is composed of nucleation and growth. The nucleation step will end as the solvent, 2-ethoxyethyl acetate evaporates. The growth step requires the moisture to migrate, something that is very slow for thick film and, therefore, the possibility exists for biuret and allophanate formation inside the bulk of the polymer [50,51]. Less T_{min} value after a certain cure time for thicker films than the thinner film was observed and suggests that phase mixing for a thick film was less. This phenomenon could be associated with the less NCO conversion for thick film, because the NCO group consumption rate in the form of biuret and allophanate is very less at 25 °C as explained earlier. We have also observed that ΔH and width in the enthalpy transition after a certain cure time was less for thick film. In order to minimize the unwanted side product formation, thin films (0.15 mm) were casted for the evaluation, and assuming that there are no side reactions, the only source of enthalpy during network growth arise from urea network formation. The fractional isocyanate conversion is estimated as [14]:

$$\rho_{NCO} = \frac{\Delta H_t}{\Delta H_\infty} \quad (2)$$

where ΔH_t and ΔH_∞ are the enthalpy values after the cure time t, and complete cured materials, respectively.

The correlation between the isocyanate conversion calculated from DSC measurements and infrared spectroscopy data for PTMG/TMP/TDI (NCO:OH = 1.6:1) system is within ± 5%. Fig. 6 shows the change in enthalpy for different moisture cure polyurethane films with cure time. The difference in the cure behavior is attributed to the difference in the cohesive forces of attraction between the polymer chains due to structural variation. The transition from an initially homogeneous state into a microphase mixed state could be affected by composition, phase constrains, crystallinity, crosslinking, and phase size effects. Also the phase mixing phenomenon and the constrain effects, due to cured diffusion layer near polymer air interface and morphological interplay, may take an important part of the behavior of enthalpy relaxation phenomenon. The results suggest that the cure rate of PTMG/TMP/TDI was more and PEG/TMP/TDI was less when we compare the soft segment structure. Fig. 7 shows

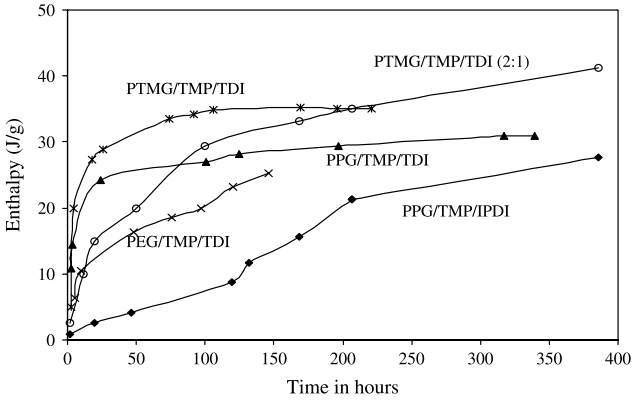

Fig. 6. Variation in enthalpy for different moisture cure PU-urea films during cure.

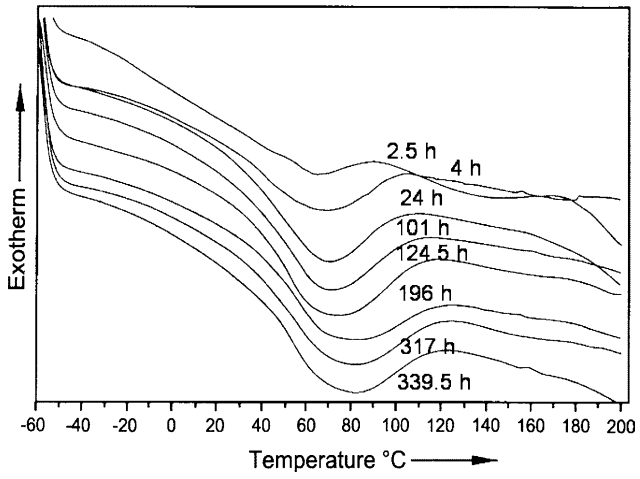

Fig. 7. DSC thermogram of PPG/TMP/TDI (NCO:OH ratio of 1.6:1) system with cure time shows the changes in T_{min} and ΔH. The T_{min} and ΔH values after 2.5 and 339.5 h were 63.9 °C, 10.9 J g^{-1} and 80.5 °C, 32.0 J g^{-1}, respectively.

the DSC thermograms of PPG/TMP/TDI (NCO:OH ratio of 1.6:1) system with cure time. T_{min} and ΔH values of PPG/TMP/TDI after 2.5 and 339.5 h were 63.9 °C, 10.9 J g^{-1} and 80.5 °C, 32.0 J g^{-1}, respectively. The lower enthalpy values during the phase mixing of PPG/TMP/TDI (Fig. 7) in comparison with PTMG/TMP/TDI (Fig. 5) suggest lower cohesive force of attraction. The T_{min} values for PPG/TMP/TDI and PTMG/TMP/TDI after 196 h were 80.5 and 76 °C, respectively, suggest that increasing amount of polyurethane/urea–ether hydrogen bonds were formed for the former system when compared to the later. However, the comparison of enthalpy data as shown in Fig. 6 suggests the order: PTMG/TMP/TDI > PPG/TMP/TDI > PEG/TMP/TDI. As for example, the enthalpy value of the transition for PTMG/TMP/TDI after 221 h was 35.1 J g^{-1}, whereas for PPG/TMP/TDI, after 317 h, ΔH associated with the transition was 30.9 J g^{-1}. Therefore, the excess enthalpy for PTMG/TMP/TDI arised from the type 1 hydrogen bonding and produced more phase separated

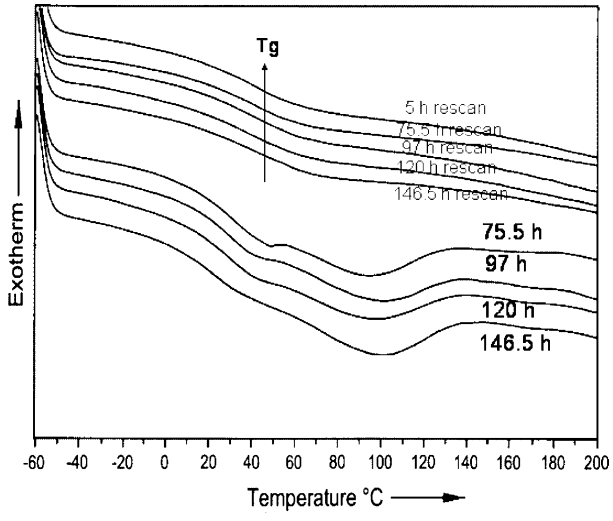

Fig. 8. DSC thermograms of PEG/TMP/TDI system with cure time. The rescanned spectra showed no change in hard segment glass transition temperature.

behavior for the completely cured PTMG/TMP/TDI system. These phenomenons could be due to the atactic nature of PPG, which is amorphous and mixes more readily with the hard segment, than PTMG. The T_{min} value of the endothermic peak for PTMG/TMP/TDI after 221 h of cure time was 87 °C, whereas for PEG/TMP/TDI (Fig. 8) system it was 102 °C after 146.5 h, suggests that more number of hydrogen bonds formed in between polyurethane/urea and ether groups for PEG based system and, therefore, its higher phase mixing characteristics than does PTMG based system. The better hydrophilic nature of PEG due to its high O/C ratio produced increased phase mixing behavior than does PTMG and PPG. Therefore, the phase mixing property follows the order: PEG > PPG > PTMG.

The results of diisocyanate structure (Figs. 4, 6 and 7) on the cure rate shows that IPDI based polyurethane takes longer time for the network growth and the phase mixing rate of TDI based MCPU was fast. For example, the T_{min} and ΔH values after 2.5 h of cure for PPG/TMP/TDI and PPG/TMP/IPDI were 63.9 °C, 10.9 J g^{-1} and 59.7 °C, 0.9 J g^{-1}, respectively. Though the % unreacted NCO groups per g in the former system was less than the other (because of more NCO group consumption in the liquid state reaction) but its more T_{min} and ΔH values suggests high reactivity as well as more phase mixing characteristics. Scheme 3 depicts the reaction of TDI and IPDI with hydroxyl functional reactants at the reaction condition and the product mixture after six hours of reaction contains diurethane (DU), monourethane as well as unreacted diisocyanate [24].

As the percentage of diisocyanate content was increased (Figs. 5 and 9), ΔH associated with the transition increased

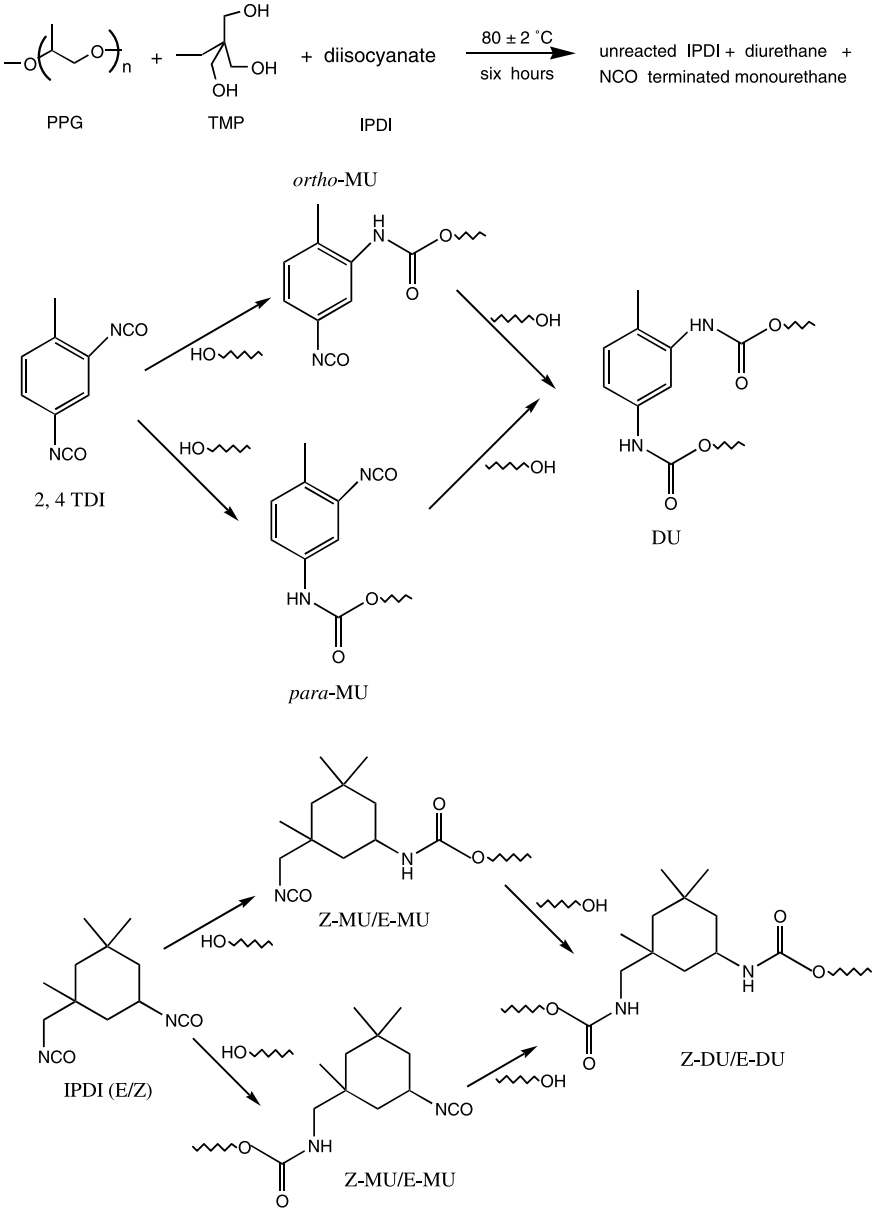

Scheme 3. Reaction of diisocyanate with other reactants in the liquid state.

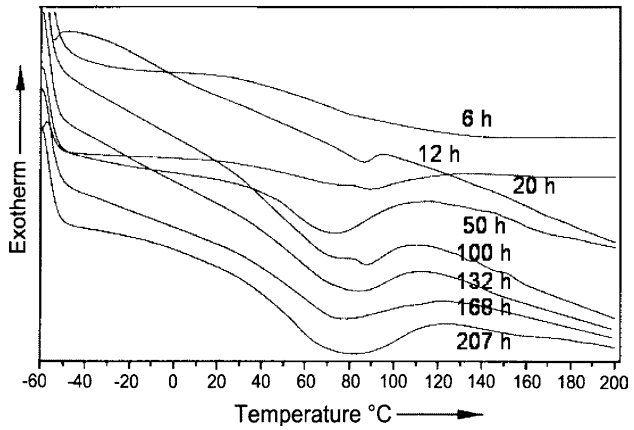

Fig. 9. DSC thermogram of PTMG/TMP/TDI (NCO:OH ratio of 2:1) system with cure time shows the changes in T_{min}, ΔH and transition breadth. The T_{min} and ΔH values after 6 and 207 h were 72.6 °C, 8.2 J g^{-1} and 83.3 °C, 35.2 J g^{-1}, respectively.

after a particular cure time. For example ΔH value of PTMG/TMP/TDI (NCO:OH = 1.6:1) after 221 h was 35.1 J g^{-1}, whereas for PTMG/TMP/TDI (NCO:OH = 2:1) it was 35.2 J g^{-1} after 207 h. This change suggests that there may be increased interaction between the hard and soft segments as the hard segment content was increased. Therefore, with increasing NCO:OH ratio, the cure rate was decreased (Fig. 6) whereas the complete cured material showed more cohesive force of attraction. This phenomenon could be due to the higher hard segment content in the material, which is equivalent to higher hard segment molecular weight in the sample. Thus an increase in hard segment content may cause more short-range order and thereby an increase in transition width, ΔH and cohesive force of attraction [52,53].

The effect of chain extender structure for PTMG/TMP/TDI (NCO:OH = 2:1) prepolymer on the phase separation behaviour is shown in Fig. 10. Under similar set of curing conditions, BEP produced slow growth of the hard domains than BD. Though it is expected that the branched chain structure of BEP may lead to more free volume and thereby may produce diffusion of water vapour easier through the barrier layer and results in enhancement in the cure rate at a particular humidity level and temperature. But its lower

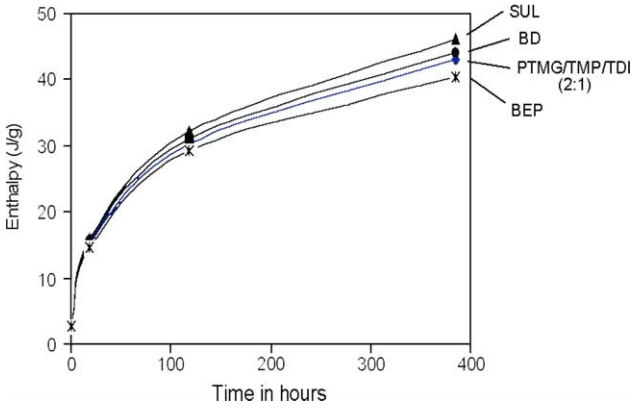

Fig. 10. Changes in enthalpy for PTMG/TMP/TDI (NCO:OH = 2:1) films chain extended with different chain extenders.

enthalpy values at any time during cure as shown in Fig. 10, suggests that the branching structure could have resulted in steric retardation towards the cohesive forces of attraction between the polymer chains. On the other hand, the polar nature of sulphone group in SUL favours faster nucleation and maturation. Since the polarity and hydrogen bonding capability (type I, Scheme 2) of SUL chain extended polyurea unit is higher compared to other chain extended polyurea units investigated, thermal stabilization of phase structures and the extent of phase separation after a certain cure time are expected to be higher in the SUL [54]. Therefore, different degree of phase mixing and morphology will be formed in the completely cured materials depending on the chain extender structure. The enthalpy data suggests that, for the completely cured materials, 4,4′-dimethyl diphenyl sulphone and 1,4-butanediol formed more cohesive force of attraction between the polymer chains and thus produced a better balance of phase separation and phase mixing characteristics. The polar groups in SUL participate in intermolecular interaction and compensate to some extent for the disadvantage of reduction in polymer symmetry due to the use of IPDI and TMP. The lower degree of cohesive attraction in BUE chain extended MCPU was due to the use of branched bulky butyl and ethyl groups in its structure, which allows moisture penetration easily from the first diffusion layer after the initial cure but hinders type 1 hydrogen bonding interaction.

These set of experimental evidences highlights the importance of the confinement effects on the phenomenology of the enthalpy relaxation due to first diffusion layer that formed near polymer–air interface after initial cure. Therefore, the reactivity difference is presumably associated with difference in the average structural/dynamical environment in the isocyanate moieties of these samples. Macroscopic water penetration into the sample should have occurred with roughly the same efficiencies unless significant difference in the morphology of these samples existed after a certain degree of cure. Hence, the observed differences in the free isocyanate reactivities in different oligomer were due to the structural difference (chemical and morphological) associated with the initial cure behavior of these samples.

3.3. Dynamic mechanical analyses

The degree of phase mixing is the most important criterion for the determinations of overall sample mechanical properties. The development of geometrically anisotropic arrangement due to structural variation may lead to different amount of connectivity and dramatically alter the solid state property of the postcure materials. Increasing interconnectivity between the chains through chemical crosslinking during cure results in enhancement of glassy modulus of the sample, as shown in Fig. 11.

The tensile storage modulus E' is a measure of the stiffness of a material and the change of modulus at 45 °C with time depicts the change in crosslink density and molecular weight build up due to crosslinking. Initially, the casted films after complete solvent evaporation were in soft condition with less

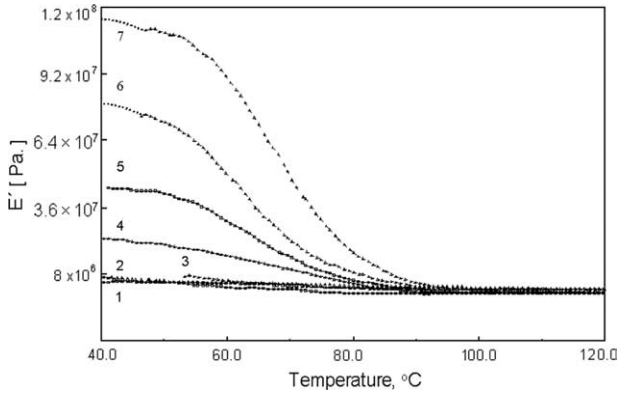

Fig. 11. The representative DMTA spectra of PTMG/TMP/TDI (NCO:OH = 1.6:1) with cure time.

storage modulus (E') at 45 °C. With time, films developed strength as a result of –NCO and moisture reaction. It was observed that the glassy and rubbery modulus of the complete cured PTMG/TMP/TDI (2:1) was more than PTMG/TMP/TDI (1.6:1) and this fact could be attributed to the larger intermolecular attraction as well as the presence of increased crosslinking due to the side product formation. On a comparison of the modulus development of different MCPUs, it was observed that the modulus value at 45 °C after a certain period of time follows the order: PTMG/TMP/TDI > PPG/TMP/TDI > PEG/TMP/TDI. This phenomenon was due to the decreasing amount of interconnectivity through type 1 hydrogen bonding in Scheme 2 [55]. The modulus of chain extended postcure material showed that at 45 °C, SUL was stiffer than other chain extended MCPUs. A large amount of interconnectivity between the hard domains may lead to a much higher modulus (i.e. stiffness) than a polymer without it would attain [56]. In the shear mode experiment, Fig. 12 shows the phase mixing characteristic of PTMG/TMP/TDI, where soft and hard segment T_g changed considerably with cure time. Fig. 13(a) is the G' and tan δ vs temperature plot of PTMG/TMP/IPDI/SUL completely cured polymer at different test frequencies. At low frequency the soft segment glass transition temperature was observed at −70.2 °C, which weakens with increasing frequency. The hard segment T_g appeared at 113 °C at 1 rad/s, and increases with increasing test frequency. From the Fig. 13(a), it was observed that microphase separation is weak in high frequency dynamic mechanical experiments [3,57]. Fig. 13(b) shows the G' and tan δ vs temperature plot of PEG/TMP/IPDI/SUL completely cured polymer at 1 Hz test frequency. The soft and

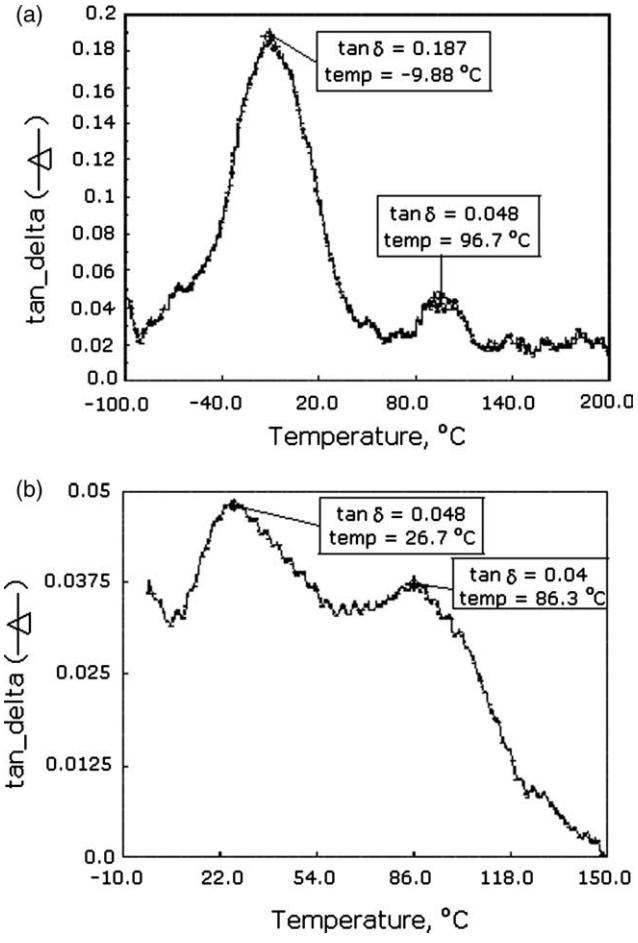

Fig. 12. The phase mixing characteristics of the representative system PTMG/TMP/TDI (NCO:OH ratio 1.6:1) after (a) 1 d and (b) complete curing. The DMTA experiment was carried out in the shear mode at 1 Hz frequency.

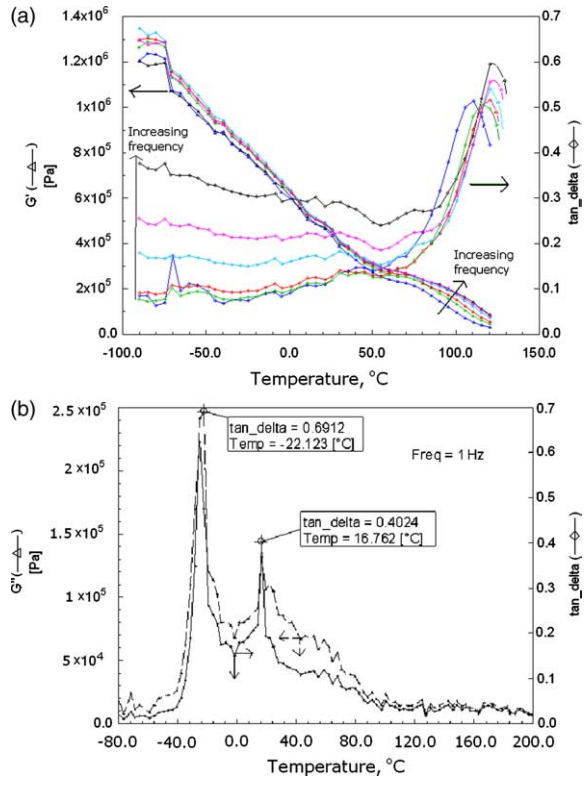

Fig. 13. Variation of G' with temperature for (a) SUL chain extended completely cured PTMG/TMP/IPDI (NCO:OH = 1.6:1) formulation in the heating process during the isochronal dynamic temperature sweep experiment at various angular frequencies (1, 5, 10, 20, 30, 40 and 80 rad/s). A single completely cured specimen of thickness 0.15 mm was employed for the entire experiment, and (b) SUL chain extended completely cured PEG/TMP/IPDI (NCO:OH = 1.6:1) MCPU.

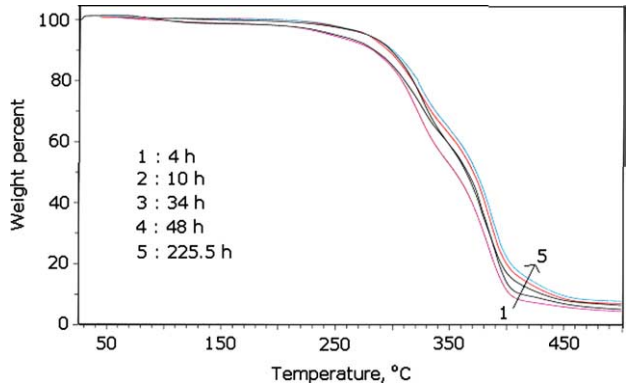

Fig. 14. The representative TG thermogram of PTMG/TMP/TDI (NCO:OH = 1.6:1) with cure time.

hard segment T_g's were appeared at −22.1 and 16.8 °C, respectively, suggests more phase mixing characteristics of PEG based formulation in compared to PTMG based formulation, PTMG/TMP/IPDI/SUL. The presence of soft segment T_g in Figs. 12(b) and 13 also supports that, in the completely cured material some amount of phase separation is also present depending on the chemical structure and produced polymers with utmost balance in properties.

3.4. Thermal stability

The representative TG curve is shown in Fig. 14. The thermal decomposition profile suggests two step decomposition patterns with the change in the stability during network maturation. The onset decomposition temperatures for the first decomposition step of PTMG/TMP/TDI (1.6:1) after 4 and 225.5 h were 270 and 295 °C, respectively. Therefore, considerable enhancement in the thermal stability with the progress of cure was achieved. Similarly substantial improvement in the decomposition onset temperature for the second stage and endset decomposition temperatures were also observed [58]. The corresponding DTG curve (not shown) showed a high temperature shift of maximum decomposition temperature (T_{max}) for both the degradation stages. At this point it is interesting to know the changes in kinetic parameters during the network maturation and whether it is possible to correlate the variation in activation energy with the degree of cure will be communicated elsewhere.

4. Conclusions

There are a large number of competing kinetic and thermodynamic factors that affect phase mixing and phase separation during the network growth for MCPUs. The structure and morphology of a set of MCPUs were investigated using mainly DSC thermograms and a novel concept was introduced to quantify the degree of cure. The results of this investigation was analyzed and correlated with the enthalpy data. The level of interconnectivity as well as cohesive force of attraction between chains is sensitive to soft segment, hard segment and chain extender structure, and is the key factor responsible for the difference in the endotherm and modulus of the postured materials. The bulky chain extender BEP disrupt the close packing of the urea groups and change the short range ordering interactions in the hard segment, whereas SUL enhance the ionic forces and results in more cohesive force of attraction and results better phase separation. Morphology of the initial diffusion layer that results after initial cure has a strong influence on moisture diffusion, thereby regulating reaction rate. An increase in NCO:OH ratio as well as use of IPDI as a diisocyanate instead of TDI have resulted in decrease in NCO group conversion after certain cure time. For the high hard segment content, phase mixing takes longer time and the completely cured material showed more cohesive force of attraction. The broadening of the enthalpy value, the increasing T_{min} and the transition width, increasing modulus and thermal stability, should be related to the increasing contribution of the confinement effects deriving from the amount of phase mixing characteristics.

Acknowledgements

We thank Dr Helena Janik, Gdansk University of Technology, Poland for helpful discussion and comments on the manuscript and DK Chattopadhyay acknowledges University Grant Commission (UGC), India for the financial support in the form of a research fellowship.

References

[1] Gisselfalt K, Helgee B. Macromol Mater Eng 2003;288:265.
[2] Heintz AM, Duffy DJ, Hsu SL, Suen W, Chu W, Paul CW. Macromolecules 2003;36:2695.
[3] Chattopadhyay DK, Sreedhar B, Raju KVSN. Ind Eng Chem Res 2005; 44:1772.
[4] Kogon IC. J Org Chem 1959;24:83.
[5] Querat E, Tighzert L, Pascault JP, Dusek K. Angew Makromol Chem 1996;242:1.
[6] Koscielecka A. Acta Polymerica 1991;42:221.
[7] Kordomenos PI, Kresta JE, Frisch KC. Macromolecules 1987;20:2077.
[8] Nierzwicki W, Wysocka E. J Appl Polym Sci 1980;25:739.
[9] Thames SF, Boyer PC. J Coat Technol 1990;62:51.
[10] Spirkova M, Kubin M, Dusek K. J Macromol Sci Chem 1990;A27:509.
[11] Cui Y, Chen D, Wang X, Tang X. Int J Adhes Adhes 2002;22:317.
[12] Dzierza W. J Appl Polym Sci 1978;22:1331.
[13] Sasaki N, Yokoyama T, Tanaka T. J Polym Sci, Polym Chem Ed 1973;11: 1765.
[14] Li W, Ryan AJ, Meier IK. Macromolecules 2002;35:6306.
[15] Elwell MJ, Ryan AJ, Grunbauer HJM, Van Lieshout HC. Macromolecules 1996;29:2960.
[16] Sanchez-Adsuar MS. Int J Adhes Adhes 2000;20:291.
[17] Aaserud Ni H, Simonsick DJ, Soucek Jr MDWJ. Polymer 2000;41:57.
[18] Petrovic ZS, Javni I. J Polym Sci, Part B: Polym Phys 1989;27:545.
[19] Chattopadhyay DK, Sreedhar B, Raju KVSN. J Appl Polym Sci 2005;95: 1509.
[20] Chattopadhyay DK, Sreedhar B, Raju KVSN. J Polym Sci, Part B: Polym Phys 2006;44:102.
[21] Yanjun C, Ling H, Xinling W, Xiaozhen T. J Appl Polym Sci 2003;89: 2708.
[22] Comyn J, Brady F, Dust RA, Graham M, Haward A. Int J Adhes Adhes 1998;18:51.
[23] Jeong YG, Hashida T, Hsu SL, Paul CW. Macromolecules 2005;38:2889.

[24] Prabhakar A, Chattopadhyay DK, Jagadeesh B, Raju KVSN. J Polym Sci, Part A: Polym Chem 2005;43:1196.
[25] Yaseen M, Raju KVSN. Prog Org Coat 1982;10:125.
[26] Coleman MM, Lee KH, Skrovanek DJ, Painter PC. Macromolecules 1986;19:2149.
[27] Mido Y. Spectrochim Acta 1972;28A:1503.
[28] Bermudez VZ, Carlos LD, Alcacer L. Chem Mater 1999;11:569.
[29] Romanova V, Begishev V, Karmanov V, Kondyurin A, Maitz MF. J Raman Spectrosc 2002;33:769.
[30] Matsui T. Chem Eng J 2002;89:143.
[31] Clough SB, Schneider NS. J Macromol Sci Phys 1968;B2:553.
[32] Saymour RW, Cooper SL. Macromolecules 1973;6:48.
[33] Crawford DM, Bass RG, Haas TW. Thermochim Acta 1998;323:53.
[34] Seymour R, Cooper S. Polym Lett 1971;9:689.
[35] Leung LM, Koberstein JT. Macromolecules 1986;19:706.
[36] Seymour RW, Cooper SL. J Polym Sci, Part B: Polym Phys 1971;9: 689.
[37] Bandekar J, Klima S. J Mol Struct 1991;263:45.
[38] Sun H. Macromolecules 1993;26:5924.
[39] Bandekar J, Klima S. Spectrochim Acta 1992;48A:1363.
[40] Tao HJ, Fan CF, MacKnight WJ, Hsu SL. Macromolecules 1994;27:1720.
[41] Ren Z, Ma D, Yang X. Polymer 2003;44:6419.
[42] Lee HS, Wang YK, Hsu SL. Macromolecules 1987;20:2089.
[43] Tanaka T, Yokoyama T, Yamaguchi Y. J Polym Sci 1968;6:2137.
[44] Coleman MM, Skrovanek DJ, Hu JB, Painter PC. Macromolecules 1988; 21:59.
[45] Petrovic ZS, Javni I, Divjakovic V. J Polym Sci, Part B: Polym Phys 1998; 36:221.
[46] Duff DW, Macial GE. Macromolecules 1991;24:387.
[47] Dusek K, Spirkova M, Havlicek I. Macromolecules 1990;23:1774.
[48] Petrovic ZS, Javni I. J Polym Sci, Part B: Polym Phys 1989;27:545.
[49] Desilets S, Villeneuve S, Laviolette M, Auger M. J Polym Sci, Part A: Polym Chem 1997;35:2991.
[50] Desilets S, Villeneuve S, Laviolette M, Auger M. J Polym Sci, Part A: Polym Chem 1997;35:2991.
[51] Pegoraro M, Galbiati A, Ricca G. J Appl Polym Sci 2003;87:347.
[52] Chen TK, Chui JY, Shieh TS. Macromolecules 1997;30:5068.
[53] Wang LF, Su KS, Wang EC, Chen JS. J Appl Polym Sci 1997;64:539.
[54] Liaw DJ, Huang CC, Liaw BY. Polymer 1998;39:3529.
[55] Park JH, Park KD, Bae YH. Biomaterials 1999;(20):943.
[56] Kaushiva BD, Wilkes GL. Polymer 2000;41:6981.
[57] Velankar S, Cooper SL. Macromolecules 2000;33:395.
[58] Chattopadhyay DK, Prasad PSR, Sreedhar B, Raju KVSN. Prog Org Coat 2005;54:296.